Spectroscopy and upconversion mechanisms of $CsCdBr_3:Dy^{3+}$

Markus Wermuth, Toni Riedener, and Hans U. Güdel
Departement für Chemie, Universität Bern, Freiestrasse 3, CH-3000 Bern 9, Switzerland
(Received 18 August 1997)

The upconversion luminescence of a Dy^{3+}-doped system is presented and analyzed. $CsCdBr_3$:x% Dy^{3+} ($x=0.2,1,5$) was synthesized and grown as crystals using the Bridgman technique. Dy^{3+} ions preferentially enter this host as charge-compensated dimers. Due to the low-phonon energy the efficiency of multiphonon-relaxation processes is significantly reduced in this host compared to oxides and fluorides. Yellow-green upconversion luminescence originating from $^4F_{9/2}$ can be induced upon excitation into $^6F_{5/2}$ or $^6F_{3/2}$ in the near infrared (NIR). Depending on the excitation wavelength, upconversion occurs by an energy-transfer or excited-state absorption mechanism. The two are distinguished by their temporal behavior after an excitation pulse. Analysis of the upconversion-luminescence transient of $CsCdBr_3$:0.2% Dy^{3+} at 10 K leads to a rate constant $W_t=165\ s^{-1}$ for the energy-transfer step. This is very small, and thus upconversion based on one excitation wavelength is inefficient. In addition, the intermediate NIR level $^6F_{5/2}$ is significantly depopulated by multiphonon relaxation at room temperature. [S0163-1829(98)02208-5]

I. INTRODUCTION

The phenomenon of upconversion luminescence, i.e., photoexcitation at a certain wavelength followed by luminescence at a shorter wavelength, is quite common in compounds containing Ln^{3+} ions.[1] Especially Pr^{3+}, Nd^{3+}, Ho^{3+}, Er^{3+}, and Tm^{3+} have been incorporated in various kinds of hosts and upconversion has been demonstrated.[2–7] But virtually nothing has been reported on Dy^{3+} in this research field, apart from examples describing Dy^{3+} in combination with other rare-earth ions[8,9] or as a quencher of luminescence.[10] This is mainly due to the dense energy-level scheme of Dy^{3+}, favoring radiationless decay of excited levels by multiphonon relaxation. These relaxation processes can be suppressed in low-phonon energy hosts, such as bromides or iodides, which, on the other hand, are not ideal from a materials point of view, due to their moisture sensitivity.

The inertness of $CsCdBr_3$ towards moisture is quite unique among the potential low-phonon energy host lattices for lanthanide ions. It crystallizes in the hexagonal system and is built up from infinite linear chains of face sharing $[CdBr_6]^{4-}$ octahedra along the crystallographic c axis. $CsCdBr_3$ has been extensively used as a host lattice for trivalent transition-metal and lanthanide ions.[2,4–6,11,12] Based on electron paramagnetic resonance and optical spectroscopy evidence, it was found that trivalent ions preferentially enter the lattice by forming a dimer unit Ln^{3+}-vacancy-Ln^{3+} replacing three Cd^{2+} ions along the chain.[11,12] Besides this energetically most favorable charge compensation, the following minority sites were postulated: Ln^{3+}-Ln^{3+}-vacancy and an isolated Ln^{3+} ion accompanied by a Cs^+ vacancy.[5] The Ln^{3+}-Ln^{3+} separation in the majority dimer is about 6 Å giving rise to weak exchange interactions and quite efficient energy-transfer processes.

In this paper we present the near infrared (NIR) to visible (VIS) upconversion-luminescence study of a Dy^{3+}-doped system. The observed upconversion in Dy^{3+}-doped $CsCdBr_3$ is spectrally and temporally analyzed. The relevant upconversion mechanisms can thus be identified and the rate constants for the important steps determined.

II. EXPERIMENT

Synthesis

$DyBr_3$ was prepared from Dy_2O_3 (Johnson & Matthey, 99.99%) following the ammoniumhalide route.[13,14] 2.55 g (6.84 mmol) of Dy_2O_3 and 4.69 g (47.8 mmol) of NH_4Br (Merck, 99.8%.) were dissolved in concentrated HBr solution (Fluka, pa. 48%) and evaporated to dryness. The obtained $(NH_4)_3DyBr_6$ was further dried under N_2 at 200 °C for 1 h followed by decomposition under vacuum at 420 °C for 3 h to obtain $DyBr_3$. For purification, the product was sublimed three times. CsBr (Merck, 99.5%) was dried under vacuum and $CdBr_2$ (Johnson and Matthey, 99%) was purified by twofold sublimation.

Using stoichiometric amounts of CsBr, $CdBr_2$, and $DyBr_3$, crystals of $CsCdBr_3$:x% Dy^{3+} (nominally $x=0.2,1,5$) were grown in silica ampoules by the Bridgman technique. Due to the hygroscopic nature of the starting materials, handling had to be carried out in a dry box. The 0.2% and 1% crystals were of good optical quality, not sensitive towards moisture and could easily be cleaved along the c axis, allowing spectroscopic measurements without polishing of crystal surfaces. The crystal nominally doped with 5% Dy^{3+} was of significantly poorer optical quality and absorption spectra indicated an effective concentration of 3.8% Dy^{3+} within the sample.

Spectroscopy

Absorption spectra were recorded on a Cary 5e (Varian) spectrometer. Continuous-wave upconversion-luminescence spectra were obtained using an argon-ion laser (Spectra Physics 2045) pumped Ti:sapphire laser (Schwartz Electro-optics) in standing-wave configuration. Wavelength control was achieved by an inchworm driven (Burleigh PZ 501) birefringent filter. The sample luminescence was dispersed

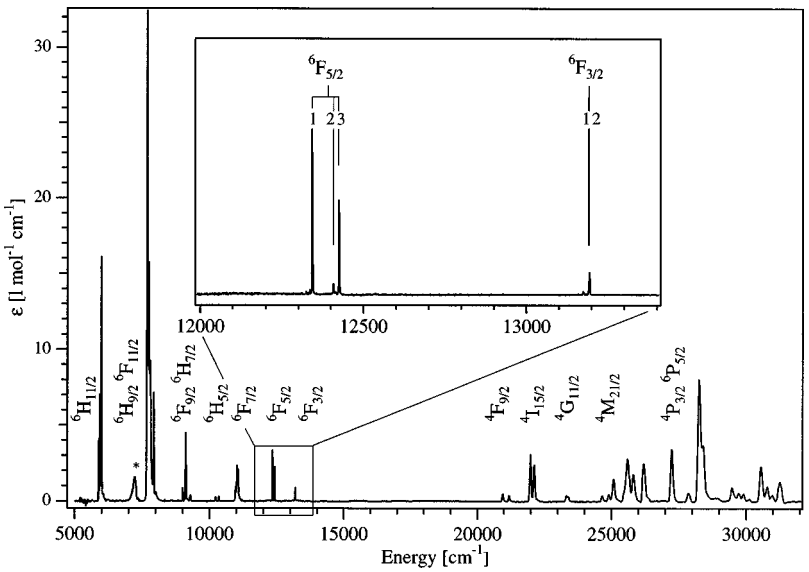

FIG. 1. Unpolarized survey absorption spectrum of $CsCdBr_3$:5% Dy^{3+} at 20 K. The asterisk denotes a water absorption. Above 20 000 cm^{-1} the bands are not fully resolved. In the high-energy region only a few selected transitions are assigned. The multiplets $^6F_{5/2}$ and $^6F_{3/2}$ are enlarged in the inset. These were used as excitation levels for upconversion experiments.

by a 0.85-m double monochromator (Spex 1402) and detected by a cooled photomultiplier (RCA 31034) using a photocounting system (Stanford Research 400).

For pulsed upconversion-luminescence measurements at the $^6F_{5/2}$ excitation energy of 12 338 cm^{-1} the output of a frequency-doubled Nd:YAG (yttrium aluminum garnet) laser (Quanta Ray DCR 3, 20 Hz) pumped dye laser (Lambda Physik FL 3002, rhodamine-101 in methanol) was Raman-shifted (Quanta Ray RS-1, H_2 340 psi). For $^4F_{9/2}$ excitation at 20 945 cm^{-1}, the dye rhodamine-B was used and the output was anti-Stokes shifted. The sample luminescence was dispersed by a 0.75-m monochromator (Spex 1702) and detected as described above. For time-resolved measurements a multichannel scaler (SR 430) was used.

Sample cooling was achieved using the helium-gas flow technique for luminescence experiments or a closed-cycle cryostat (Air Products) for absorption measurements.

Luminescence spectra were corrected for the sensitivity of the detection system. They are displayed as photon counts versus energy (cm^{-1}).

III. RESULTS

Figure 1 shows the absorption spectrum of $CsCdBr_3$:5% Dy^{3+} in the spectral region between 5000 and 32 000 cm^{-1} at 20 K. It consists of weak and narrow lines, characteristic of f-f transitions. The assignment is straightforward from a comparison with the literature.[15] In the high-energy region only some selected multiplets are assigned. The energy gap between the sextet and quartet states is 7000 cm^{-1}. The spectrum is dominated in intensity by the transition $^6H_{15/2} \rightarrow {}^6H_{9/2}/{}^6F_{11/2}$ around 8000 cm^{-1}. The transition to $^6F_{1/2}$ expected around 13 750 cm^{-1} is too weak to be observed in the survey spectrum, confirming the selection rule that allows only transitions with $\Delta J \leqslant 6$. The inset shows the multiplets $^6F_{5/2}$ and $^6F_{3/2}$ that were excited for upconversion-luminescence studies. The energies of the most important crystal-field levels obtained from high-resolution absorption spectra and used in the subsequent upconversion studies are summarized in Table I. The f-f energy-level scheme of Dy^{3+} is shown in Fig. 2. The total splitting of the

TABLE I. Selected energy levels for $CsCdBr_3$:Dy^{3+} extracted from high-resolution absorption and luminescence spectra; energies are given in cm^{-1}.

$^6H_{15/2}$	(1)	0	$^6F_{9/2}$	(1)	8994.4	$^4M_{21/2}$	(1)	24 615
	(2)	17		(2)	9004.1		(2)	24 631
	(3)	31		(3)	9105.0		(3)	24 633
	(4)	153		(4)	9108.3		(4)	24 648
	(5)	264		(5)	9123.3		(5)	24 861
	(6)	308	$^6F_{5/2}$	(1)	12 339		(6)	24 887
	(7)	359		(2)	12 405		(7)	24 944
	(8)	381		(3)	12 421		(8)	25 024
$^6H_{13/2}$	(1)	3545	$^6F_{3/2}$	(1)	13 186		(9)	25 046
	(2)	3552		(2)	13 189		(10)	25 065
	(3)	3556	$^4F_{9/2}$	(1)	20 912		(11)	25 080
	(4)	3566		(2)	20 933	$^4I_{13/2}$	(3)	25 454
	(5)	3573		(3)	20 945		(4)	25 456
	(6)	3577		(4)	21 171		(5)	25 520
	(7)	3587		(5)	21 176		(6)	25 553

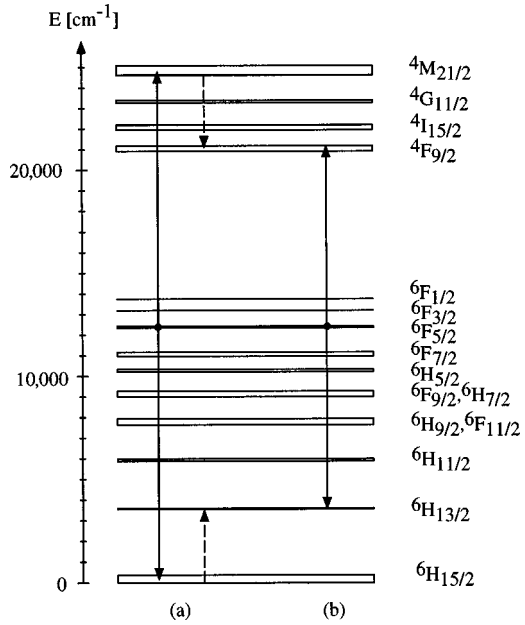

FIG. 2. Energy-level diagram of Dy^{3+} with two possible ETU mechanisms to populate $^4F_{9/2}$ after $^6F_{5/2}$ excitation. The cross-relaxation step is indicated with dashed arrows.

multiplets by the crystal field is indicated by the height of the boxes.

Figure 3 presents the upconversion-luminescence spectrum in the VIS and near ultraviolet of $CsCdBr_3$:1% Dy^{3+} at 10 K under continuous-wave $^6F_{5/2}$ excitation at 12 338 cm^{-1}. A comparison with energy differences between individual crystal-field levels obtained from high-resolution absorption spectra leads to the assignments given in the figure. The $^4F_{9/2}\rightarrow{}^6H_{13/2}$ transition is dominant, determining the yellow-green color of the upconversion luminescence. In addition to the transitions originating from $^4F_{9/2}$ weak luminescence transitions from $^4M_{21/2}$ and $^4P_{3/2}$ can be detected. The total intensity of the upconversion luminescence decreases by about two orders of magnitude between 10 K and room temperature. The power dependence for $^4F_{9/2}$ and $^4M_{21/2}$ luminescence intensities is exactly quadratic, indicating a two-photon process to populate the emitting level. The $^4P_{3/2}$ luminescences show a cubic power dependence; this emitting level lies at an energy of 27 148 cm^{-1} that cannot be reached by absorption of two 12 338-cm^{-1} photons and is thus populated by a three-photon process.

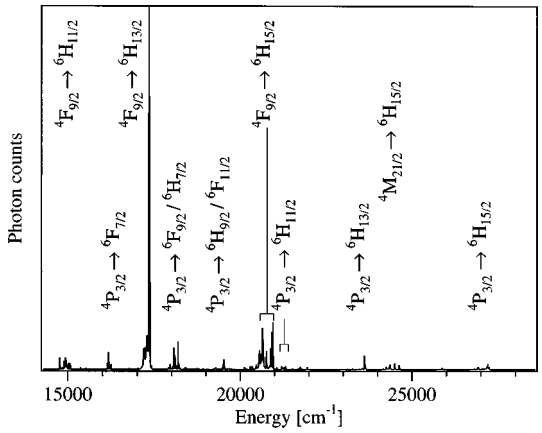

FIG. 3. Survey upconversion-luminescence spectrum of $CsCdBr_3$:1% Dy^{3+} at 10 K using $^6F_{5/2}$ excitation at 12 338 cm^{-1}, see Fig. 1.

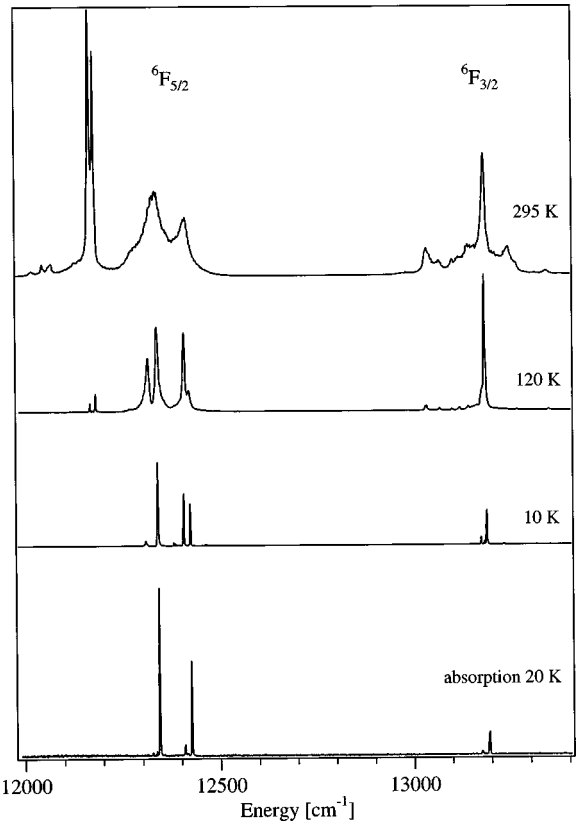

FIG. 4. Upconversion-excitation spectra of $CsCdBr_3$:1% Dy^{3+} at three temperatures detecting the intense $^4F_{9/2}\rightarrow{}^6H_{13/2}$ luminescence at 17 341 cm^{-1}. The individual spectra are scaled to an equal height of the peak at 12 338 cm^{-1}. The absorption spectrum at 20 K of the same spectral region is shown at the bottom.

Excitation spectra monitoring the upconverted $^4F_{9/2}\rightarrow{}^6H_{13/2}$ luminescence at 17 341 cm^{-1} of $CsCdBr_3$:1% Dy^{3+} at three different temperatures are shown in Fig. 4. Below 20 K the similarity of the excitation spectrum to the corresponding absorption spectrum that is shown for comparison is evident. With increasing temperature, the excitation lines get broader and there arise intense and extraordinarily sharp lines at 12 164 cm^{-1} and 12 177 cm^{-1}. The intensity of these lines relative to the excitation line at 12 338 cm^{-1} increases by factors of 2 and 4 when going from the 0.2% sample to the 1% and 5% sample, respectively. Also at 13 181 cm^{-1} another hot line is observed.

Figure 5 shows the decay of the $^4F_{9/2}$ luminescence intensity after pulsed excitation into $^4F_{9/2}$ of $CsCdBr_3$:0.2% Dy^{3+} at 10 K. The semilogarithmic plot reveals a double-exponential decay curve. From a double-exponential fit we obtain decay times of 105 and 501 μs for the two branches, with two orders of magnitude more intensity in the fast part. This behavior is reproducible for different excitation intensities and Dy^{3+} concentrations. The $^4F_{9/2}$ lifetime of the majority site is attributed to the dominant first part (105 μs). The slowly decaying part is attributed to a minority center with a lifetime of 501 μs. In $CsCdBr_3$:Tb^{3+} a similar relation

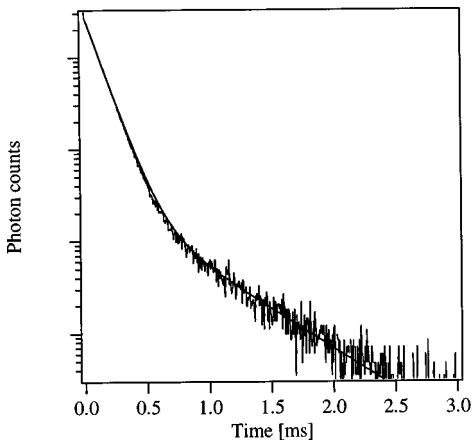

FIG. 5. $^4F_{9/2} \rightarrow {}^6H_{13/2}$ luminescence decay after $^4F_{9/2}$ excitation of $CsCdBr_3$:0.2% Dy^{3+} at 10 K. The ordinate scale is logarithmic. The excitation pulse has a width of 10 ns and occurs at $t=0$. The data were fitted with a double exponential decay function.

of luminescence lifetimes belonging to different centers has been found.[16]

The upconversion-luminescence transients of $^4F_{9/2}$ obtained under pulsed $^6F_{5/2}$ excitation of $CsCdBr_3$:Dy^{3+} at 10 K are shown in Figs. 6(a) and 6(b) for 0.2% and 1% Dy^{3+}, respectively. The luminescence intensity is seen to slowly build up after the excitation pulse. The maximum is reached

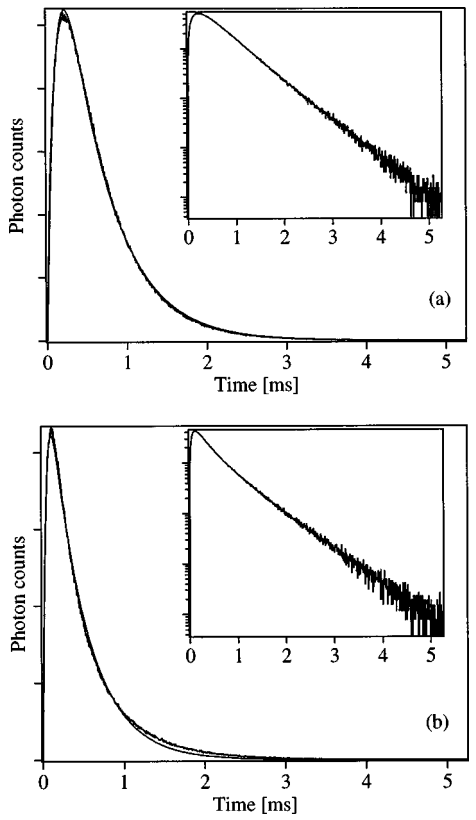

FIG. 6. (a) $^4F_{9/2} \rightarrow {}^6H_{13/2}$ upconversion-luminescence transient after $^6F_{5/2}$ excitation (12 338 cm^{-1}) of $CsCdBr_3$:0.2% Dy^{3+} at 10 K. The excitation pulse has a width of 10 ns and occurs at $t=0$. The smooth line corresponds to a fit with Eq. (5). The inset shows the same data in a semilogarithmic plot. (b) Same transient for $CsCdBr_3$:1% Dy^{3+}.

TABLE II. Luminescence rise and decay times extracted from time-dependent measurements at 10 K. The values are given in μs. Calculated data are obtained using the Judd-Ofelt model (see Sec. IV A).

		Expt.		Calc.	
Excitation	Detection	Rise	Decay	Decay	conc.
$^6F_{5/2}$	$^6F_{5/2}$		1200	744	0.2%
$^4F_{9/2}$	$^4F_{9/2}$		105	222	0.2%
$^6F_{5/2}$	$^4F_{9/2}$	107	546		0.2%
	$^6H_{13/2}$			10 000	
$^6F_{5/2}$	$^4F_{9/2}$	41	426		1%

at about 210 and 120 μs for the 0.2% and 1% samples, respectively, and then we observe a decay within a few milliseconds. From the semilogarithmic plots in the inset of Fig. 6 we see that the decay is perfectly single exponential in the dilute sample but shows a small deviation in the concentrated one. An analysis in terms of a rise and decay time, which will be discussed in detail in Sec. IV C, yielded the following respective results: 107 and 546 μs for the 0.2% crystal, 41 and 426 μs for the 1% crystal.

The luminescence rise and decay times at 10 K extracted from the time-dependent experiments are collected in Table II. Whereas the lifetime of $^6F_{5/2}$ is strongly temperature dependent—it decreases from 1.2 ms at 10 K to 250 μs at room temperature—the value of the $^4F_{9/2}$ lifetime is not significantly affected by temperature changes.

IV. DISCUSSION

A. Upconversion luminescence and lifetimes of excited states

In view of the fact that no upconversion luminescence has been reported so far in a purely Dy^{3+}-doped system our observation of visible luminescence upon NIR excitation is remarkable and deserves analysis. Upconversion processes require, among other factors, the availability of an intermediate state with a sufficiently long lifetime, so that a high population of this state can be achieved. The energy-level scheme of Dy^{3+} in Fig. 2 is characterized by a relatively dense packing of multiplets in the near infrared. This is followed by a large energy gap of about 7000 cm^{-1} separating the highest sextet $^6F_{1/2}$ from the lowest quartet $^4F_{9/2}$. The quartet states again show a relatively dense packing. This energy-level structure largely determines whether and under what conditions upconversion processes can occur.

The lifetime of an excited state is determined by both radiative and nonradiative depopulation processes. The radiative rate constants are largely determined by the electronic structure of the lanthanide ion; their dependence on the coordination geometry and the chemical nature of the coordination is of minor importance. The same is not true for multiphonon-relaxation processes. They depend on the energies of the accepting phonon modes, and for lanthanide systems the so-called energy-gap law can be used to express the multiphonon-relaxation rate constant w_0:[17]

$$w_0 = \beta e^{-\alpha p}. \quad (1)$$

In Eq. (1) α and β are parameters characteristic of the material, $p=\Delta E/\hbar\omega$ is the number of phonons of energy $\hbar\omega$ required to bridge the electronic energy gap ΔE. The highest-energy phonons are the most efficient accepting modes. According to a rule of thumb for f-f states in lanthanides, multiphonon relaxation is dominant for $p<5$. This rule has a sound empirical and theoretical basis.[3,18] Highest-energy phonons in oxides, fluorides, chlorides, and bromides have typical energies of ~ 600, ~ 400, ~ 260, and $\sim 160\ \mathrm{cm}^{-1}$, respectively. For $CsCdBr_3$ a value of $163\ \mathrm{cm}^{-1}$ was determined by Raman spectroscopy.[19]

The large energy gap of $7000\ \mathrm{cm}^{-1}$ between the quartet and sextet states of Dy^{3+} prevents an efficient $^4F_{9/2} \rightsquigarrow {}^6F_{1/2}$ multiphonon relaxation even in oxides. Thus, if an upconversion process can be achieved, a luminescence from the lowest quartet states is likely to occur. The problem is to obtain a sufficiently long lifetime of the intermediate sextet level in the NIR. The largest energy gap of Dy^{3+} in the NIR (see Fig. 2) is about $1300\ \mathrm{cm}^{-1}$ between $^6F_{5/2}$ and $^6F_{7/2}$. With the maximum phonon energies quoted above, $p<5$ for both oxides and fluorides, and multiphonon relaxation $^6F_{5/2} \rightsquigarrow {}^6F_{7/2}$ is thus very competitive. The same is of course true for all the other gaps between 14 000 and 9000 cm^{-1}, which are all smaller than the $^6F_{5/2}$-$^6F_{7/2}$ gap. The situation is very different for the $CsCdBr_3$ host chosen in the present study. p is about eight for the $^6F_{5/2}$-$^6F_{7/2}$ gap, and the rate constant for multiphonon relaxation is smaller by orders of magnitude than in an oxide or a fluoride. This, in our opinion, accounts for the nonobservation of Dy^{3+} upconversion luminescence so far.

The experimentally determined lifetime $\tau=1.2$ ms at 10 K of $^6F_{5/2}$ for $CsCdBr_3$:0.2% Dy^{3+} confirms that nonradiative quenching cannot be important. We used a Judd-Ofelt analysis to estimate the radiative contribution to the experimental lifetime.[20,21] In a Judd-Ofelt calculation three intensity parameters $\Omega_{(\lambda)}$ ($\lambda=2,4,6$) are fitted to oscillator strengths f extracted from unpolarized room-temperature absorption spectra, using the following formula:

$$f=\frac{8\pi^2 m\nu}{3h}\frac{\chi}{(2J+1)} \times \sum_{\lambda=2,4,6} \Omega_{(\lambda)} |\langle f^n SLJ \| \mathbf{U}^{(\lambda)} \| f^n S'L'J' \rangle|^2. \quad (2)$$

In Eq. (2) χ stands for the local-field correction. For electric-dipole induced absorption and emission processes it is related by the following expressions to the refractive index n, respectively:

$$\chi_{\mathrm{abs}}=\frac{(n^2+2)^2}{9n}, \quad (3)$$

$$\chi_{\mathrm{em}}=\frac{n(n^2+2)^2}{9}. \quad (4)$$

The refractive index n was set to 1.78.[4] The last factor in Eq. (2) is the square of a reduced matrix element of the tensor operator $\mathbf{U}^{(\lambda)}$, characteristic of a transition between the multiplets $|f^n SLJ\rangle$ and $|f^n S'L'J'\rangle$ within the f^n electron configuration. These elements are determined by the four atomic parameters $F^{(2)}$, $F^{(4)}$, $F^{(6)}$, and ζ.[22] The $\Omega_{(\lambda)}$ parameters obtained from fitting absorption intensities can in turn be used to calculate oscillator strengths and rate constants of transitions between excited states. From the sum of all radiative decay-rate constants the radiative lifetime of a given multiplet is then obtained.

TABLE III. Comparison of experimental with calculated oscillator strengths for $CsCdBr_3$:Dy^{3+}. The values used as input for the least-squares procedure are indicated in boldface. The following fit parameters were used: $\Omega_{(2)}=2.48\times10^{-19}\ \mathrm{cm}^2$, $\Omega_{(4)}=2.29\times10^{-20}\ \mathrm{cm}^2$, $\Omega_{(6)}=5.98\times10^{-21}\ \mathrm{cm}^2$.

Transition	f_{obs} (10^{-6})	f_{calc} (10^{-6})
$^6H_{15/2} \rightarrow {}^6\mathbf{H}_{11/2}$	**1.64**	1.72
$\rightarrow {}^6H_{9/2}/{}^6F_{11/2}$	19.8	22.3
$\rightarrow {}^6F_{9/2}/{}^6H_{7/2}$	0.619	1.81
$\rightarrow {}^6\mathbf{H}_{5/2}$	**0.008**	0.002
$\rightarrow {}^6\mathbf{F}_{7/2}$	**0.656**	0.916
$\rightarrow {}^6\mathbf{F}_{5/2}$	**0.338**	0.290
$\rightarrow {}^6\mathbf{F}_{3/2}$	**0.050**	0.054
$\rightarrow {}^6F_{1/2}$		0.00
$\rightarrow {}^4\mathbf{F}_{9/2}$	**0.134**	0.089
$\rightarrow {}^4\mathbf{G}_{11/2}$	**0.185**	0.137

As no data for $F^{(2)}$, $F^{(4)}$, $F^{(6)}$, and ζ were available for $CsCdBr_3$:Dy^{3+}, these atomic parameters were estimated in the following way: Their values are known for $CsCdBr_3$:Er^{3+} and for both Er^{3+} and Dy^{3+} in LaF_3.[23,24] Assuming the same ratio of these atomic parameters for Er^{3+} and Dy^{3+} in the two lattices, the following values were derived for $CsCdBr_3$:Dy^{3+}: $F^{(2)}=91\,877\ \mathrm{cm}^{-1}$, $F^{(4)}=66\,486\ \mathrm{cm}^{-1}$, $F^{(6)}=45\,106\ \mathrm{cm}^{-1}$, $\zeta=1892\ \mathrm{cm}^{-1}$.

This fixed set of parameter values was then used to determine $\Omega_{(\lambda)}$ by fitting Eq. (2) to the 295-K absorption intensities of the multiplets. Only the oscillator strengths of multiplets that are well separated could be used as input values for the least-squares procedure. These multiplets are given in boldface in Table III. The table shows that the experimentally determined values are very well reproduced over the whole range of four orders of magnitude by Eq. (2). The intensity parameters $\Omega_{(\lambda)}$ thus obtained were used to calculate radiative lifetimes of various excited states. A comparison of calculated and measured lifetimes is given in Table II. For $^6F_{5/2}$ the measured lifetime at 10 K is found to be somewhat longer than the calculated one. We conclude that nonradiative processes play a negligible part in the depopulation of $^6F_{5/2}$ at this temperature. The observed decrease of $\tau(^6F_{5/2})$ from 1200 to 250 μs between 10 and 295 K, which is accompanied by a corresponding decrease in the luminescence intensity is attributed to thermally activated nonradiative processes such as multiphonon relaxation or the cross-relaxation process $^6F_{5/2}+{}^6H_{15/2} \rightarrow {}^6F_{9/2}+{}^6H_{13/2}$, indicated with dashed arrows in Fig. 7. This latter process is thermally activated because the gap between $^6H_{15/2}(1)$ and $^6H_{13/2}(1)$ is greater by $200\ \mathrm{cm}^{-1}$ than the gap between $^6F_{5/2}(1)$ and $^6F_{9/2}(1)$; compare Table I.

For the other important multiplet $^4F_{9/2}$ the measured and calculated lifetimes at 10 K differ by a factor of 2. This lies

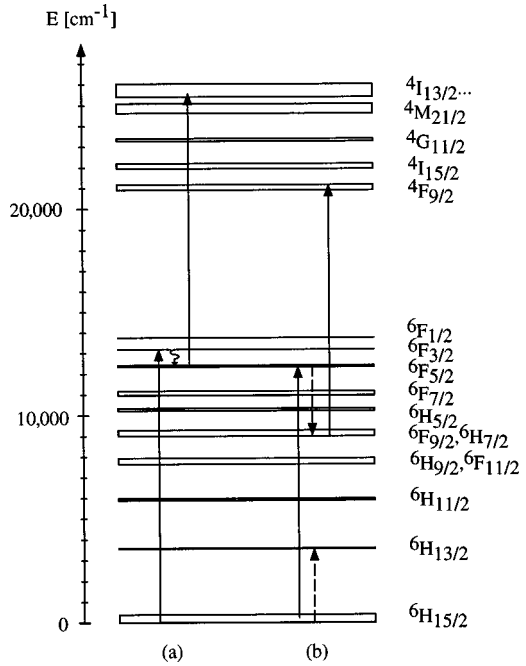

FIG. 7. Energy-level diagram of Dy^{3+} with two possible ESA mechanisms after excitation into $^6F_{3/2}$ (a) and $^6F_{5/2}$ (b), respectively. The cross-relaxation step preceding ESA is indicated with dashed arrows, the multiphonon-relaxation step with a curly arrow.

within the accuracy of the Judd-Ofelt procedure, and we conclude that the experimental $\tau = 105\ \mu$s is essentially radiative.

B. Upconversion mechanisms

The long lifetime of $^6F_{5/2}$ for $CsCdBr_3$:Dy^{3+} is favorable for upconversion processes involving this multiplet after NIR excitation. $^6F_{3/2}$ excitation also leads to $^6F_{5/2}$ population by a fast multiphonon relaxation across the small energy gap corresponding to 4.7 high-energy phonons. This is confirmed by the fact that even at 10 K no $^6F_{3/2}$ luminescences can be induced by direct excitation into this multiplet. Thus upconversion-luminescence spectra always look similar, independent of which of the two multiplets, $^6F_{5/2}$ or $^6F_{3/2}$, is originally pumped by the excitation source.

Basically, upconversion can occur by two different processes, radiatively by an excited-state absorption (ESA) or nonradiatively by an energy-transfer upconversion (ETU) between two excited ions.[1,25] A distinction of the two mechanisms can often be made on the basis of energy arguments. Energy-transfer processes are most efficient when the exciting laser is resonant with a ground-state absorption. The energy-transfer step itself can then be phonon assisted. The efficiency of an ESA upconversion process is determined by both the radiative ground-state and the excited-state absorption step. We therefore often find efficient upconversion when the laser is resonant with the second step, i.e., the ESA step. A clear distinction between ETU and ESA processes is possible by their different time evolution after an excitation pulse of a few ns width.[26,27] The radiative ESA process occurs within the pulse width leading to an immediate decay of the upconversion-luminescence intensity after excitation, whereas the nonradiative ETU process is characterized by an observable rise after the laser pulse, followed by a decay. This distinction is possible when the pulse width is much shorter than the time constant of the relevant energy-transfer step.

The upconversion-luminescence transient, obtained under pulsed $^6F_{5/2}$ excitation (Fig. 6) clearly shows the latter behavior. It will now be analyzed in terms of possible energy-transfer upconversion processes. Starting from $^6F_{5/2}$, two ETU mechanisms for the population of the dominant emitting multiplet $^4F_{9/2}$ are energetically possible. They are shown in Fig. 2: In the first process (a), the whole $^6F_{5/2}$ excitation energy is transferred, leading to a population of $^4M_{21/2}$. Inspection of the energy levels in Table I shows that the process $^6F_{5/2}(1)+{}^6F_{5/2}(1)\rightarrow{}^6H_{15/2}(3)+{}^4M_{21/2}(4)$ is resonant to within one wavenumber. The numbers in brackets designate the crystal-field levels of the respective multiplet. Because $^4M_{21/2}$ is separated by eight high-energy phonons from $^4G_{11/2}$, multiphonon relaxation to $^4F_{9/2}$ is not efficient. In order to explain the predominant $^4F_{9/2}$ upconversion luminescence, a subsequent cross-relaxation step $^4M_{21/2}+{}^6H_{15/2}\rightarrow{}^4F_{9/2}+{}^6H_{13/2}$ has to be included in the pathway [see dashed arrows in Fig. 2(a)]. Supporting evidence for this cross relaxation was found in the luminescence spectra directly excited into $^4M_{21/2}$, which show strong $^4F_{9/2}$ emission and only very weak $^4M_{21/2}$ emission. $^4F_{9/2}$ can also be populated by an ETU process in which only the energy difference between $^6F_{5/2}$ and $^6H_{13/2}$ is transferred [Fig. 2(b)]. This process is nonresonant. It releases at least 187 cm^{-1} into the phonon system. The relative importance of the processes (a) and (b) in Fig. 2 cannot be evaluated on the basis of energy arguments alone. However, the analysis of the time-dependent measurements presented in Sec. IV C will allow a clear distinction: The mechanism 2(b) will turn out to be dominant.

The most striking features of the upconversion-excitation spectra in Fig. 4 are the prominent hot lines at 12 164, 12 177, and 13 181 cm^{-1}. From their temperature dependence they obviously correspond to a thermally activated process. The 13 181-cm^{-1} line corresponds to the energy difference between $^6F_{5/2}(1)$ and $^4I_{13/2}(5)$ and is therefore assigned to the ESA process (a) in Fig. 7. Despite the fact that the ESA step originates in $^6F_{5/2}(1)$ it is overall a thermally activated process for the following reason. The energy difference between the excited-state absorption and the ground-state absorption step $^6H_{15/2}(1)\rightarrow{}^6F_{3/2}(1)$ is 5 cm^{-1}. This is significantly larger than the homogeneous linewidth at 10 K, and thus the process is not resonant and not efficient. At 120 and 295 K the situation is completely different. Homogeneous linewidths exceed 5 cm^{-1} and the efficiency of the ESA upconversion process increases by at least two orders of magnitude; see Fig. 4.

The situation is more complicated and more interesting for the very prominent 12 164- and 12 177-cm^{-1} excitation lines in Fig. 4. With their sharpness even at 295 K they show the typical behavior of ESA excitations. Analysis of Table I shows that the two lines match the energy differences $^6F_{9/2}(1)\rightarrow{}^4F_{9/2}(4)$ and $^6F_{9/2}(2)\rightarrow{}^4F_{9/2}(4)$, respectively. In assigning the two lines to these ESA transitions we have the supporting Judd-Ofelt calculation which gives a high oscillator strength of 2.1×10^{-6} for the $^6F_{9/2}\rightarrow{}^4F_{9/2}$ transition. But how do we obtain $^6F_{9/2}$ population in the first place? The ground-state absorption step $^6H_{15/2}\rightarrow{}^6F_{5/2}$ must be fol-

lowed by a very efficient cross-relaxation step $^6F_{5/2}+{}^6H_{15/2}\rightarrow{}^6F_{9/2}+{}^6H_{13/2}$ as shown by the dashed arrows in Fig. 7(b). This process is energetically favorable, and it is supported by the following important nonobservation. The two lines at 12 164- and 12 177-cm^{-1} are missing in an upconversion excitation spectrum using 10-ns pulse excitation, whereas the other upconversion excitations can be performed by pulsed or cw excitation. This is in excellent agreement with our postulated upconversion mechanism at these two energies, in which the ESA step is preceded by a nonradiative cross-relaxation step, which is slow compared to the excitation-pulse width. The latter cannot take place within the 10 ns of the laser pulse, and thus the sequence of steps is only possible if the pulse width is at least of the same order of magnitude as the time constant of the intermediate cross-relaxation step. This condition is obviously fulfilled in the limit of cw excitation, where a steady-state $^6F_{9/2}$ population is created. The 12 164- and 12 177-cm^{-1} lines in the cw upconversion-excitation spectrum increase in intensity with increasing Dy^{3+} concentration, in excellent agreement with a concentration-dependent cross-relaxation step in the mechanism.

C. Dynamics of upconversion

The observed rise in Fig. 6 of the upconversion-luminescence transients after pulsed $^6F_{5/2}$ excitation is a fingerprint for an ETU process. Energy transfer can occur by electric multipole or exchange interactions, which are both strongly distance dependent.[28,29] Therefore in host lattices with a statistical distribution of dopant ions a whole range of transfer-rate constants is usually contained in such transients, thus complicating the analysis of experimental data. If trivalent rare-earth ions are doped in low concentration into $CsCdBr_3$, pair centers with a well-defined shortest ion-ion separation of about 6 Å are predominantly formed.[11] Therefore, the energy transfer behavior should be dominated by the intradimer transfer processes as long as energy migration between the dimers can be neglected. This greatly simplifies the analysis, and the intradimer process should be represented by a single transfer rate constant W_t. In the following analysis W_t will be determined.

Buisson and Vial have analytically analyzed a dimer situation in terms of rate equations.[30] This procedure was then applied to extract energy-transfer rate constants from upconversion-luminescence transients of $CsCdBr_3:Er^{3+}$.[2] The situation is schematically represented for a three-level system in Fig. 8. The following processes are included in the model: Both ions of the dimer are initially excited to the intermediate state 2. State 3 is subsequently populated by an energy-transfer step with a rate constant W_t. State 3 will then decay to both states 2 and 1. Because the branching to state 2 does not lead to a situation from which state 3 can be repopulated by a further upconversion step within the isolated ion pair, this branching is omitted in the analysis and W_3 represents the total relaxation of state 3. As both ions in state 2 can decay individually to the ground state and as the excitation of the partner ion is lost for an upconversion process after one ion has decayed, the rate constant W_2 has to be multiplied by a factor of 2 in the rate equation.

The system of linear differential equations resulting from these assumptions can be solved analytically, leading to the following temporal behavior of the population N_3 of state 3 after excitation of both ions into state 2:[30]

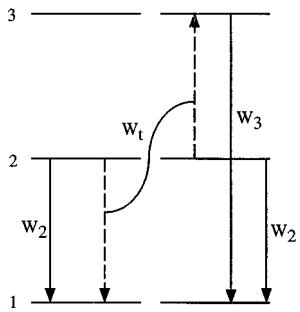

FIG. 8. Schematic three-level system for the isolated ion-pair model with rate constants for the relevant processes. Radiative and nonradiative processes are indicated by full and broken arrows, respectively.

$$N_3(t)=k(e^{-(2W_2+W_t)t}-e^{-W_3t}). \tag{5}$$

In this difference of two exponentials, the bigger exponent determines the rise of the transient, whereas the smaller one determines the decay. One time constant corresponds directly to W_3 and the other one contains both $2W_2$ and the transfer-rate constant W_t. For a determination of W_t we require independent measurements or estimates of W_2 and W_3, the decay-rate constants of the intermediate and final levels in a single ion, respectively. This is possible for $CsCdBr_3:Dy^{3+}$ as shown below.

Of the two possible mechanisms (a) and (b) in Fig. 2 the mechanism (b) will emerge as the correct one in the analysis. For this mechanism the levels 1, 2, and 3 of Fig. 8 can be assigned to $^6H_{13/2}$, $^6F_{5/2}$, and $^4F_{9/2}$, respectively. The fit of Eq. (5) to the 10-K upconversion transient of the $CsCdBr_3$:0.2% Dy^{3+} crystal in Fig. 6(a) is excellent. The inset of the figure shows that the decay part is perfectly single exponential over three orders of magnitude. The rise and decay times of 107 and 546 μs, respectively, can now be assigned to W_3 and $2W_2+W_t$ or vice versa. The luminescence lifetimes of $^6F_{5/2}$ and $^4F_{9/2}$ at 10 K determined by direct excitation are 1200 and 105 μs, respectively; see Table II. We can thus immediately assign the *rise* time of the upconversion transient to the *decay* of $^4F_{9/2}$: $W_3=1/105\ \mu s=9520\ s^{-1}$. The decay part of the transient is then attributed to the decay of the intermediate level and the energy-transfer process: $2W_2+W_t=1/546\ \mu s=1830\ s^{-1}$. Inserting $W_2=1/1200\ \mu s$ we obtain for the energy-transfer rate constant $W_t=165\ s^{-1}$.

The alternative mechanism (a) in Fig. 2 would lead to a transient consisting of three exponential terms with individual prefactors, two of them describing the feeding of $^4F_{9/2}$ and one describing the decay. This transient could not be fitted by Eq. (5). This alternative mechanism to populate $^4F_{9/2}$ is therefore ruled out by the temporal behavior of the upconversion-luminescence intensity.

In $CsCdBr_3:Er^{3+}$ transfer-rate constants determined by a similar analysis have been reported for several upconversion processes.[2] W_t values range from 128 to 1942 s^{-1}. Our $W_t=165\ s^{-1}$ for $CsCdBr_3$:0.2% Dy^{3+} is at the lower end of this

range. The ET upconversion process is thus very inefficient and just barely competitive with other radiative and nonradiative processes in our system.

The upconversion transient of the $CsCdBr_3$:1% Dy^{3+} crystal [Fig. 6(b)] shows some small but significant deviations from the ideal behavior of the more diluted system. Both the rise and the decay are somewhat faster and the decay is no longer purely single exponential. We attribute these deviations to the onset of energy migration, particularly in the long-lived intermediate state $^6F_{5/2}$. Evidence for energy migration at a doping level of 1% has been reported for $Cs_3Lu_2Br_9$:Er^{3+}.[26] It generally leads to a shortening of the rise and decay times as observed here. Evidence for the onset of energy-transfer processes between dimers is also provided by the observed enhancement in the concentrated crystal of the ESA upconversion induced by the lines at 12 164 and 12 177 cm^{-1}, which requires a cross-relaxation between dimers.

V. CONCLUSIONS

The choice of a low-phonon energy host lattice is crucial for obtaining upconversion in a Dy^{3+}-doped crystal. This is due to the particular energy-level structure of Dy^{3+}. In high-energy phonon hosts the lifetimes and thus populations of potential intermediate states are reduced by multiphonon relaxation, thus reducing the probability of upconversion processes.

The present study demonstrates the feasibility of NIR to VIS upconversion in Dy^{3+}-doped $CsCdBr_3$. Due to the dimer structure of the Dy^{3+} centers in diluted $CsCdBr_3$ a perfect match is obtained between the observed upconversion transient after pulsed excitation and a very simple dimer model. The transfer-rate constant $W_t = 165\ s^{-1}$ for the energy-transfer upconversion step within the dimer is very small, and thus upconversion is not competitive with other deactivation processes, particularly at higher temperatures.

Despite the fact that $CsCdBr_3$:Dy^{3+} is insensitive to moisture, its potential as an upconversion material is small. The situation might change significantly, however, if two exciting lasers could be tuned to the most efficient ground- and excited-state absorption steps. We are presently exploring the use of two tunable laser sources.

ACKNOWLEDGMENTS

We thank M. Hehlen for providing his Judd-Ofelt program. Financial support by the Swiss National Science Foundation and the Priority Program ''Optics'' of the Board of Swiss Federal Institutes of Technology is acknowledged.

[1] F. E. Auzel, Proc. IEEE **61**, 758 (1973).
[2] N. J. Cockroft, G. D. Jones, and D. C. Nguyen, Phys. Rev. B **45**, 5187 (1992).
[3] T. Riedener, K. Krämer, and H. U. Güdel, Inorg. Chem. **34**, 2745 (1995).
[4] J. Neukum, N. Bodenschatz, and J. Heber, Phys. Rev. B **50**, 3536 (1994).
[5] C. Barthou and R. B. Barthem, J. Lumin. **46**, 9 (1990).
[6] M. Mujaji, G. D. Jones, and R. W. G. Syme, Phys. Rev. B **48**, 710 (1993).
[7] T. Riedener, H. U. Güdel, G. C. Valley, and R. A. McFarlane, J. Lumin. **63**, 327 (1995).
[8] J. Ohwaki and M. Otsuka, Electron. Lett. **31**, 752 (1995).
[9] J. Ohwaki and Y. Wang, Appl. Phys. Lett. **65**, 129 (1994).
[10] Y. Seki, Rev. Elec. Commun. Lab. **20**, 1103 (1972).
[11] G. L. McPherson and L. M. Henling, Phys. Rev. B **16**, 1889 (1977).
[12] G. L. McPherson, W. M. Heung, and J. J. Barraza, J. Am. Chem. Soc. **100**, 469 (1978).
[13] J. B. Reed, B. S. Hopkins, and L. F. Audrieth, Inorg. Synth. **1**, 28 (1978).
[14] G. Meyer, Inorg. Synth. **25**, 146 (1989).
[15] F. S. Richardson, M. F. Reid, J. J. Dallara, and R. D. Smith, J. Chem. Phys. **83**, 3813 (1985).
[16] P. A. M. Berdowski, M. J. J. Lammers, and G. Blasse, J. Chem. Phys. **83**, 476 (1985).
[17] L. A. Riseberg and H. W. Moos, Phys. Rev. **174**, 429 (1968).
[18] J. M. F. van Dijk and M. F. H. Schuurmans, J. Chem. Phys. **78**, 5317 (1983).
[19] O. Pilla, E. Cazzanelli, B. Blanzat, C. Andraud, and F. Pellé, Phys. Status Solidi B **144**, 845 (1987).
[20] B. R. Judd, Phys. Rev. **127**, 750 (1962).
[21] G. S. Ofelt, J. Chem. Phys. **37**, 511 (1962).
[22] S. Hüfner, *Optical Spectra of Transparent Rare-Earth Compounds* (Academic, New York, 1978).
[23] J. R. Quagliano, N. J. Cockroft, K. E. Gunde, and F. S. Richardson, J. Chem. Phys. **105**, 9812 (1996).
[24] W. T. Carnall, G. L. Goodman, K. Rajnak, and R. S. Rana, J. Chem. Phys. **90**, 3443 (1989).
[25] J. C. Wright, Top. Appl. Phys. **15**, 239 (1976).
[26] M. P. Hehlen, G. Frei, and H. U. Güdel, Phys. Rev. B **50**, 16 264 (1994).
[27] T. Riedener and H. U. Güdel, J. Chem. Phys. **107**, 2169 (1997).
[28] Th. Förster, Ann. Phys. (Leipzig) **2**, 55 (1948).
[29] D. L. Dexter, J. Chem. Phys. **21**, 836 (1953).
[30] R. Buisson and J. C. Vial, J. Phys. (Paris) Lett. **42**, L115 (1981).